KERNFORSCHUNGSZENTRUM

KARLSRUHE

Mai 1965

KFK 301
SM 62/1

Institut für Angewandte Kernphysik

A Review of Pulsed Neutron Experiments on Non-Multiplying Media

K. H. Beckurts

GESELLSCHAFT FÜR KERNFORSCHUNG M. B. H.

KARLSRUHE

KERNFORSCHUNGSZENTRUM KARLSRUHE

Mai 1965

KFK 301
SM 62/1

Institut für Angewandte Kernphysik

A Review of Pulsed Neutron Experiments on Non-Multiplying Media

K.H. Beckurts

Gesellschaft für Kernforschung m.b.H. Karlsruhe

INTERNATIONAL ATOMIC ENERGY AGENCY

SYMPOSIUM ON PULSED NEUTRON RESEARCH

May 10 - 14, 1965
Kernforschungszentrum Karlsruhe, Germany

SM 62/1

A REVIEW OF PULSED NEUTRON EXPERIMENTS ON NON-MULTIPLYING MEDIA

K. H. Beckurts
Kernforschungszentrum Karlsruhe

1. Introduction

For the last twelve years, there has been an increasing interest in the use of pulsed sources techniques for the study of neutron migration, thermalization and absorption in matter. For instance, about twenty different determinations of the diffusion parameters of ordinary water and ice, more than thirty experiments on various "organic" moderators - many of them as a function of temperature - and nine experiments on graphite have been published. Many of the data determined in this way are in disagreement and it appears doubtful if their use in reactor design has justified this big effort. There is no doubt, however, that these studies have - probably more than any other class of experiments - contributed to improve our understanding of the kinetic behaviour of neutrons in matter. In particular, they have stimulated important developments in transport and thermalization theory some of which will be reviewed at this conference /1/. Furthermore, neutron kinetics studies with pulsed sources have proved to be a useful - and rather inexpensive - field for student training and in fact a growing percentage of the work is being carried out at university laboratories. Finally, the good success which the pulsed source technique is having for reactivity determinations on reactor systems would probably not have been encountered without the important developments in instrumentation and analysis techniques achieved during the early studies on non-multiplying media.

In this paper we shall try to summarize some recent developments in this field, especially to review the progress made since the last major international conference which was held at Brookhaven in 1962 /2/. We shall mainly deal with decay measurements on thermalized neutron fields (section 2) to which by far the biggest research activity has been devoted. In section 3, transient phenomena in moderators - i.e. experiments to measure slowing-down and thermalization times - will be considered. Section 4 will deal with the fairly new field of "quasi-asymptotic" decay of monoenergetic neutron fluxes in heavy scattering substances.

This is not a reporter type conference, and a considerable number of individual contributions are to be presented. In order not to anticipate too much the following papers we shall restrict ourselves to areas which will not be otherwise covered. The paper will therefore be far from a complete survey.

2. The Decay of a Thermalized Neutron Field

Under certain limitations, which are now fairly well understood theoretically /3/, a thermalized neutron field in a moderator is in a true asymptotic state and decays strictly exponentially with time. The classical approach is to measure the time constant α of this decay and to correlate it with the geometrical buckling B^2 of the assembly. The resulting α vs. B^2 curve is analysed in terms of the diffusion parameters of the moderating material. Instead of varying the size of the system, one also can vary the concentration N of an added non-1/v absorber; analysing the resulting α vs. N curve yields parameters characteristic for the thermalization properties of the scattering medium. There are closely related stationary techniques, i.e. measurement of the diffusion length as a function of concentration of a 1/v or non-1/v absorber. The α vs. B^2 method is hampered by three basic difficulties: The first of them is a purely experimental one, viz., the precise determination of α in the presence of non-asymptotic neutrons and background. The second problem is a theoretical one and consists in the calculation of the geometrical buckling from the given dimensions of the scattering medium. Thirdly, there is the problem of analysing the α vs. B^2 curve properly. The difficulty to define the geometrical buckling does not necessarily arise in α vs. N or stationary poisoning experiments since they can be performed on nearly infinite media. The other two problems, however, arise in both latter techniques in an analogous form.

2.1 Problems arising in α determinations.

Due to their extremely good thermalization properties, an asymptotic spectrum is rapidly established in hydrogenous moderators. "Waiting time" problems thus do not seriously effect α measurements if care is taken to eliminate higher spatial modes. Room return background can be annoying but the assemblies can be easily shielded since they tend to be quite small. Another source of background, as noted by Silver /4/, may be photoneutrons from the decay of 7.35 sec N^{16} produced by the $O^{16}(n,p)N^{16}$ reaction on the oxygen present in water. This reaction has a threshold at 9.6 MeV and will occur if the neutron source employs the $H^3(d,n)He^4$ reaction. Other authors did not find this background troublesome; it can completely be eliminated by use of a $H^2(d,n)He^3$ or other low energy neutron source. Using lower energy sources has the advantage that shielding against room return neutrons becomes simpler, and it is for this reason that Ogrzewalski et al. /5/ used a fast chopper at a research reactor as a neutron source. It should be kept in mind, however, that the elimination of higher spatial modes will be the more difficult the lower the source neutron energy is.

The situation is quite different in crystaline moderators like beryllium and graphite where the trapping of low energy neutrons creates a serious limit beyond which the decay constant cannot grow. This limiting value, $\lim_{v \to o} v \cdot \Sigma_t$, is about 2600 sec^{-1} in graphite and 3800 sec^{-1} in beryllium; the corresponding critical values of the buckling are about $15 \cdot 10^{-3}$ cm^{-2} and $40 \cdot 10^{-3}$ cm^{-2}, respectively. The above figures for $\lim_{v \to o} v \cdot \Sigma_t$ are based on very old measurements of the scattering cross section below the Bragg cutoff and may therefore be greatly in error /6/. Nevertheless, it is obvious that at very high bucklings no clean asymptotic mode will exist. This is borne out in Fig. 1 where the decay of the neutron density in a beryllium block of $B^2 = 73 \cdot 10^{-3}$ cm^{-2} is plotted according to Fullwood, Slovacek and Gaerttner /7/. The decay is nearly exponential at times between 300 and 700 /usec after the pulse injection but tends to be slower later on. In order to demonstrate that the latter effect cannot be attributed to improper background substraction, these authors measured in the same setup the neutron decay in a polyethylene assembly whose size was chosen to give approximately the same decay rate. This showed up to be purely exponential as may be seen in Fig. 1. A similar experiment on a small graphite stack was performed by Küchle /8/. He found a similar deviation from a pure exponential decay but the statistical accuracy of the data was not sufficient to back up any far-reaching conclusion.

Being aware of these difficulties, most recent experimenters on crystalline media have confined their measurements to the low B^2 range. They have also established criteria in order to make sure that the observed decay corresponds to a true asymptotic state. Especially, the waiting time which must elapse after the pulse injection before the evaluation of the decay curve for α may begin has been determined by several groups working on graphite [9 - 12]. Fig. 2 shows the waiting time required to obtain good exponential decay in graphite according to Serdula [12].

Recently, there is some conflicting information. Davis, de Juren and Reier [13] have used a paraffin shield around their graphite stacks in addition to the usual cadmium lining. Furthermore, their experimental area was shielded by walls of cans filled with borated water. Using a $H^2(d,n)He^3$ neutron source and collimating these neutrons directly on their graphite assemblies in order to avoid direct leakage of source neutrons into the experimental area, Davis, de Juren and Reier obtained clean exponential decay curves after waiting times of 1 msec or less even at bucklings as high as $10 \cdot 10^{-3}$ cm^{-2}. They state that "waiting times probably are an a tifact of the shielding and the initial neutron energy rather than a property of a graphite stack in space". Zhezherun et al. [14] were able to observe clean exponential decays over up to four decades in beryllium systems at bucklings up to $110 \cdot 10^{-3}$ cm^{-2}. This corresponds to α values up to 10^4 sec^{-1}, i.e. figures highly above the critical limit stated before! This is in direct contradiction to the above mentioned experiment of the R.P.I. group and also violates the critical limit theorem to an extent which would be difficult to explain from inaccuracies in the measured low energy cross section.

2.2 On the definition of the geometric buckling.

Defining the geometrical buckling is done in a most straightforward manner if the full space-time distribution can be measured and analysed in terms of Fourier modes. Such measurements are conveniently performed on rather large systems. Experiments on graphite [12, 13] have proved that the relation $d = \frac{2.13\ D_o}{\nu}$ is a very good approximation for the extrapolated endpoint, irrespective of the buckling. For very small water systems, a strong dependency of the extrapolated endpoint on the size and shape of the scattering medium is borne out by the remarkable differences in the α vs. B^2 curves measured on "flat" and on "cubic" systems [15 - 18] whose bucklings were calculated using the simple formula $d = \frac{2.13\ D_o}{\nu}$. Theoretical calculations of the extrapolated endpoint in H_2O show that it decreases with increasing B^2 due to the diffusion cooling effect [19];

these calculations have partly been verified by experiments [18]. However, in order to explain the measured discrepancies on flat and on cubic systems, the extrapolated endpoint had to increase again considerably at high bucklings. An increase of the extrapolated endpoint for very thin slabs has indeed been predicted from an exact one-group theory treatment of the one-dimensional case [20, 21]. Also, it is known that in one-group theory, in the limit of very small dimensions slabs and spheres show a quite different behaviour of the decay constant. In order to resolve the discrepancies observed on small water systems, a multigroup transport theory treatment of the three-dimensional case would be of great help. Unfortunately, direct measurements of the space - time neutron distribution in these very small systems are not possible for experimental reasons.

2.3 Analysis of α vs. B^2 measurements.

The usual prccedure of evaluating measured α vs. B^2 curves is to approximate them by an expression

$$\alpha = \overline{\nu \Sigma_a} + D_o B^2 - C B^4 + F B^6 + - \ldots \qquad (1)$$

by a least square fitting method. Some authors use weight factors on the individual α_i values (preferably $\sim 1/\alpha_i^2$) in order to take care of their varying accuracy, others do not. It has been noted several times that the diffusion parameters derived in this way may vary by several times the most probable statistical error according to the length of the B^2 interval used, the way in which weight factors were applied, or according to whether a B^6 form was included or not. This is especially the case in graphite where the α vs. B^2 curves measured by some authors were in agreement whilst the derived diffusion parameters were not. The most popular explanation for these discrepancies is that the above procedure results in a "global" fit which represents the whole measured α vs. B^2 region in the best possible way, thus not yielding necessarily the most probable diffusion parameters. Several authors have therefore used different evaluation procedures. For instance, if the absorption cross section is known, the simpler relation

$$\frac{\alpha - \overline{\nu \Sigma_a}}{B^2} = D_o - C B^2 + F B^6 + - \ldots \qquad (2)$$

is fitted to the corrected data. Other authors use iterative procedures where the weight given to an experimental point is dependent on the influence which the diffusion parameter to be determined has on α. Most of these procedures, however, do not seem to be free of ambiguities, and for the time being the author would prefer a least squares fitting according to equ. (1) with appropriate weighing of the individual points.

In view of these difficulties, the proposal has been made to compare measured α vs. B^2 curves - after the elementary correction for density and temperature deviations - directly among themselves or with the theoretically predicted curves. Apart of the fact that experimentalists will not like this proposal since they want to produce meaningful physics data instead of unanalysed curves, there are several objections against this procedure: Our main interest in these comparisons is to see the effect of diffusion cooling, i.e. the deviation of the data from the straight line behaviour. We aim at a theoretical prediction of these effects (i.e. of the coefficients C and F) to, say, 15 - 25 %. In order to realize these small differences between measured and predicted diffusion cooling by direct comparison of calculated and measured α vs. B^2 curves, the accuracy of the theoretical value of D_o must be very high, say, 1 %. This high accuracy in the theoretical prediction of D_o seems difficult to reach, especially in crystalline moderators where the scattering cross section may vary slightly according to varying grain size. For the latter reason, direct comparisons between various experimental curves may show a larger disagreement in the amount of diffusion cooling than actually exists. In liquid moderators with a well-defined chemical composition, comparisons between experimental curves are reasonable whereas comparisons with theory may be hampered by inaccurate knowledge of D_o.

2.4 Some recent data on ordinary water.

Some results of previous experiments are plotted in Fig. 3. Shown at $B^2 > 0$ are the results of pulsed experiments by Küchle [15]. At $\frac{1}{L^2}$ $(= - B^2) > 0$, the results of a careful poisoning experiment by Starr and Koppel [16] are plotted. It had been assumed so far that measurements in the upper left quadrant of this coordinate system were not possible. However, as Joest and Memmert [24] have pointed out, this region is accessible to experiments by measuring the diffusion length L in a non-stationary neutron field which is excited by a neutron source with a time behaviour $S(t) \sim e^{-\alpha t}$, $0 < \alpha < \overline{v\Sigma_a}$. Their statement is easy to prove: Assume an infinite medium with a plane source $S(t) \sim e^{-\alpha t}$ at $z = o$. Then in diffusion theory approximation, the flux $\phi(E,t,z)$ will be governed by

$$\frac{1}{v} \frac{\partial \phi(E,t,z)}{\partial t} = - v \Sigma_a \phi(E,t,z) + D(E) \frac{\partial^2 \phi(E,t,z)}{\partial z^2} + \mathcal{H} \phi + A \cdot \delta(z) e^{-\alpha t} \qquad (3)$$

where H is the thermalization operator. Since $\alpha < v\Sigma_a$, the homogenous solutions of equ. (3) will decay faster than the source term and the asymptotic time behaviour

of the neutron flux will be $\sim e^{-\alpha t}$. Putting $\Phi(E,t,z) = \Phi(E,z) \cdot e^{-\alpha t}$, we obtain

$$\left\{ v\Sigma_a - \alpha \right\} \Phi(E,z) = D(E) \frac{\partial^2 \Phi(E,z)}{\partial z^2} + \varkappa \Phi + A\,\delta(z) \qquad (4)$$

which is identical to a stationary diffusion problem in a moderator with $\Sigma_a^* = \Sigma_a - \alpha/v$. It is thus seen that the trick of using an exponentially decaying source expands the region of poisoning experiments really until $\Sigma_a^* = 0$, i.e. $\Sigma_p = -\Sigma_a$.

Arai and Küchle /23/ have recently performed measurements of this type on water. In order to realize an exponentially decaying source, they used a graphite assembly together with a large water reflector (Fig. 4). The neutrons from a 14 MeV source were injected into the graphite stack whose size was such that - after die-away of the transients - the composite system decayed with a time constant $\alpha < (v\Sigma_a)_{H_2O}$. The neutron density was measured in the H_2O as a function of distance from the graphite - H_2O interface with a small BF_3 counter. Time gates were used in order to suppress the transients. The resulting decay is exponential with distance and - after a small correction for lateral leakage - yields the diffusion length of the time-decaying neutron field. The resulting values of $1/L^2$ as a function of α are included in Fig. 3. The full curve is the result of a least-squares 4-parameter fit of all the data. The corresponding diffusion parameters are (at 20° C)

$$v\Sigma_a = 4782 \pm 15 \text{ sec}^{-1} \qquad D_o = 35{,}630 \pm 80 \text{ cm}^2\text{sec}^{-1}$$
$$C = 3420 \pm 170 \text{ cm}^4\text{sec}^{-1} \qquad F = 214 \pm 139 \text{ cm}^6\text{sec}^{-1}$$

The high statistical accuracy of these parameters indicates a good internal consistency of the data, the authors nevertheless recommend to increase the error limits by a factor of three. In table 1, these data are compared with various recent calculations of the diffusion parameters for H_2O.

Table 1 Measured and calculated diffusion parameters in H_2O at 20° C

D_o (cm^2sec^{-1})	C (cm^4sec^{-1})	F (cm^6sec^{-1})	remarks
37,045	3361	169	calculated by Ghatak and Honeck /25/ using Nelkin model
37,570	3380	210	calculated by Clendenin /26/ using Nelkin model[1)]

38,230	2730	250	calculated by Clendenin /26/ using Radkowski model [1]
37,400	3350	144	calculated by Kallfelz /27/ using Goldman - Nelkin model
33,900	3080	218	calculated by Kallfelz /27/ using the Haywood - Thorson scattering law
35,630 ± 80	3420 ± 170	214 ± 139	Experiment of Arai and Küchle /23/
35,300 ± 300	-	-	calculated by Springer et al. /29/ from $\Sigma_s(E)$ and $\bar{\mu}(E)$

From an inspection of the table, the following conclusions can be drawn [2]:

a) The diffusion cooling coefficients predicted using either the Nelkin or the Goldman-improved Nelkin model agree very well among themselves and with the prediction derived from the experimental scattering law of water. All these predictions are in good agreement with the experimental value.

b) The diffusion coefficient as predicted by the Nelkin model is about 4 - 5 % higher than the experimental value. As Koppel and Young /28/ have pointed out, the agreement between the Nelkin model prediction and the measurement of neutron cross sections and spectra in H_2O is considerably improved if the anisotropy of the molecular vibrations is accounted for in the model. Their modification of the Nelkin model reduces the predicted D_o by about 4 %, i.e. practically removes the discrepancy between experiment and theory completely!

---

1) These calculations were done at 23°C. The value of D_o was therefore decreased by 400 $cm^2 sec^{-1}$; C and F were not corrected.

2) It was shown by Arai that the experimental diffusion parameters change only very slightly if instead of Küchle's pulsed data, those of Lopez and Beyster /16/ are used. Also, no large change occurs if the region $B^2 > 0.4$ cm^{-2}, where the discrepancies in the α vs. B^2 curves have been observed, is not used for the evaluation procedure.

The diffusion coefficient as derived from the experimental scattering law for water is about 4 % lower than the directly measured value. This discrepancy is not very disturbing in view of the fact that D_o depends very critically on the low ß portion of the $S(\alpha,ß)$ function which is difficult to measure accurately. Springer et al. [29] carefully measured $\bar{\mu}(E)$, the average cosine of the scattering angle as a function of incident energy, and computed D_o from $\bar{\mu}(E)$ and $\Sigma_s(E)$ by averaging $\frac{1}{3\Sigma_s(E)(1-\bar{\mu}(E))}$ over an equilibrium Maxwellian. The result is also well compatible with the Arai and Küchle experiment.

c) The Radkowski kernel calculations predict a diffusion cooling coefficient about 12% lower and a diffusion coefficient about 8% higher than the experiment.

2.5 New data on various moderators.

Organic substances

Some data on Dowtherm A, diphenyl and benzene at room temperature are given in tables 2, 3 and 4. It is seen that for each of these moderators, there are fortunately two measurements which are in reasonably good agreement. D_o and C were calculated by Kallfelz [27] using experimental scattering law data measured by Gläser [34]. In the case of diphenyl, a value of D_o calculated from the measured $\Sigma_s(E)$ and $\bar{\mu}(E)$ by Springer et al. is also listed.

Table 2 Diffusion parameters in Dowtherm A at room temperature

$\overline{v\,\Sigma_a}(sec^{-1})$	$D_o(cm^2sec^{-1})$	$C\ (cm^4sec^{-1})$	Remarks
2870 ± 40	49,200 ± 600	11,900 ± 2100	measured by Küchle [15]
2985 ± 85	51,000 ± 1650	16,500 ± 7000	measured by Brown [18]
—	51,500	12,200	calculated by Kallfelz [27]

Table 3 Diffusion parameters in benzene at room temperature

$\overline{v\Sigma_a}$ (sec^{-1})	D_o ($cm^2 sec^{-1}$)	C ($cm^4 sec^{-1}$)	Remarks
2886 ± 111	48694 ± 1373	13869 ± 3849	measured by Pál et al. [30]
3120 ± 50[3]	48500 ± 800	13300 ± 2400	measured by Küchle and Kussmaul [31]
——	55500	8260	calculated by Kallfelz [27]

Table 4 Diffusion parameters in diphenyl at room temperature (at a density 1.053 g cm^{-3}

$\overline{v\Sigma_a}$ (sec^{-1})	D_o ($cm^2 sec^{-1}$)	C ($cm^4 sec^{-1}$)	Remarks
3700 ± 150	42,120 ± 1160	7700 ± 1800	measured by Bayer, Červená and Schäferlingova [32]
3470 ± 280	43,370 ± 1800	13,700±2900	measured by Ádám, Bod and Pál [33]
——	48,500	10,340	calculated by Kallfelz [27]
——	48,500 ± 1000	——	calculated by Springer et al. [29] from $\Sigma_s(E)$ and $\bar{\mu}(E)$

It is seen that the diffusion cooling coefficients based on the experimental scattering law are in the right order of magnitude. The values of D_o derived from the scattering law in diphenyl and benzene are about 15% too high. The reason for this discrepancy is probably the same as discussed at the end of section 2.4.

Without much further comment we mention some other recent experiments on organic moderators: Yurowa et al. [35] have performed temperature-dependent experiments over a large T range on benzene, diphenyl, diphenylmethane, diphenylether, gasoil, isopropyldiphenyl, anisole and tetradecane. From these experiments, they were able to derive a simple relationship

$$\frac{\rho}{\rho_o} D_o (T) = A \cdot T^{a/2} \qquad (5)$$

for the dependency of the diffusion coefficient D_o on the absolute temperature T. Here ρ and ρ_o are the densities of the liquid at temperatures T and T_o, respectively, whereas A and a are characteristic constants which were determined for each of the above liquids. Pál et al. [30] measured the diffusion parameters of benzene, toluene, xylene, cyclohexane, hexane at 22°C and of diphenyl at 85°C. For the same substances, they measured the total cross section as a function of energy between 2 and 100 meV and derived the diffusion coefficient by use of the

3) This would yield a microscopic absorption cross section of 348 millibarn per H atom. Presumably, impurities were present in the liquid.

classical Radkowski prescription. Agreement within better than 20 % between the calculated and measured values of D_o was found. Measurements on diphenyl at 77°C and in MIPB at 30°C were reported by Blackshaw and Waltner /36/, on liquid ammonia by Charles /37/ and on heptane between 17,5°C and 80°C by Nilsson and Sjöstrand /38/. Some new results on terphenyl and paraffin are quoted in /39/.

Graphite

Table 5 lists some more recent data on graphite.

Table 5 Diffusion parameters of graphite (1.6 density) at room temperature

D_o ($cm^2 sec^{-1}$)	C ($cm^4 sec^{-1}$)	F ($cm^6 sec^{-1}$)	Remarks	
$2.13 \pm 0.02 \cdot 10^5$	$26 \pm 5 \cdot 10^5$	——	3-par. fit $B^2 \leq 6 \cdot 10^{-3} cm^{-2}$	Exp.[4] of Klose, Küchle and Reichardt /10/
$2.11 \pm 0.02 \cdot 10^5$	$16 \pm 5 \cdot 10^5$	$-20 \pm 10 \cdot 10^7$	4-par. fit $B^2 \leq 12 \cdot 10^{-3} cm^{-2}$	
$2.14 \pm 0.01 \cdot 10^5$	$39 \pm 3 \cdot 10^5$	——	3-par. fit $B^2 \leq 18.9 \cdot 10^{-3} cm^{-2}$	Exp. of Starr and Price /9/
$2.19 \pm 0.03 \cdot 10^5$	$39 \pm 4 \cdot 10^5$	——	3-par. fit $B^2 \leq 15.4 \cdot 10^{-3} cm^{-2}$	Exp. of Sagot and Tellier /11/
$2.30 \pm 0.06 \cdot 10^5$	$45.6 \pm 4.7 \cdot 10^5$	——	3-par. fit $B^2 \leq 12.8 \cdot 10^{-3} cm^{-2}$	Exp. of Serdula /12/
$2.26 \pm 0.27 \cdot 10^5$	$34.4 \pm 38.8 \cdot 10^5$	$-6.9 \pm 17.7 \cdot 10^7$	4-par. fit $B^2 \leq 12.8 \cdot 10^{-3} cm^{-2}$	
$2.187 \pm 0.008 \cdot 10^5$	$30 \pm 1 \cdot 10^5$	——	3-par. fit $B^2 \leq 5.3 \cdot 10^{-3} cm^{-2}$	Exp.[4] of Davis, de Juren and Reier /13/
$2.20 \pm 0.009 \cdot 10^5$	$44.3 \pm 4 \cdot 10^5$	$+12.7 \pm 5 \cdot 10^7$	4-par. fit $B^2 \leq 12 \cdot 10^{-3} cm^{-2}$	
$2.178 \cdot 10^5$	$24.6 \cdot 10^5$	$-8.3 \cdot 10^7$	calculation by Honeck /40/ using Parks model	

[4] A measurement of the stationary diffusion length was included in the evaluation procedure.

All parameters have been reduced to a density of 1.6 g/cm^3. For comparison, the theoretical values predicted by Honeck /40/ on the basis of the Parks model are included. The following comments can be made on the data in this table: Apart of the data measured most recently by Davis, de Juren and Reier, the four other α vs. B^2 curves, if plotted together, are in a reasonably good agreement. The differences are essentially due to different methods of evaluation. If Klose, Küchle and Reichardt would evaluate their experiment by a three-parameter fit up to $B^2 \approx 12 \cdot 10^{-3}$cm^{-2}, they would obtain $D_o \approx 2.17 \cdot 10^5$ cm^{2}sec^{-1} and $C \approx 40 \cdot 10^5$ cm^{4}sec^{-1}, i.e. results compatible with those of the following three authors. However, Klose, Küchle and Reichardt found that a three-parameter least squares fit did not work very well above $B^2 \approx 6 \cdot 10^{-3}$cm^{-2}, i.e. above $B^2 = 6 \cdot 10^{-3}$cm^{-2}, they found a continuous increase of the value of C with the length of the B^2 interval used in the evaluation. Above $B^2 = 6 \cdot 10^{-3}$cm^{-2}, it was necessary to include a negative B^6 term in order to perform a consistent analysis. The existence of a negative B^6 term in graphite is predicted by theory; the experiments of Starr, Honeck and Villiers /41/ on the average asymptotic velocity as a function of B^2 in graphite also give strong evidence for a negative B^6 term. Neither Starr and Price nor Sagot and Tellier found it necessary to include such a term in the analysis of their α vs. B^2 curves; they used, however, a different evaluation technique than Klose, Küchle and Reichardt. The results of Serdula's analysis seem to confirm the results of Klose, Küchle and Reichardt, the statistical accuracy however is very low. Davis, de Juren and Reier have also mentioned that a 4-parameter fit is superior to a 3-parameter fit above $B^2 \approx 6 \cdot 10^{-3}$cm^{-2}. However, they report a positive B^6 term. The reason for this discrepancy is probably the fact that in this most recent determination an α vs. B^2 curve was found which looks quite different at high B^2 values. This is shown in Fig. 5 where these data are compared with those of Starr and Price. The difference in the experimental setup, as was mentioned in section 2.1, is the increased shielding and the fact that 2.5 MeV neutrons were used; the procedure was different since Davis, de Juren and Reier used short waiting times.

Summarizing, the situation in graphite appears to be still very dark, partly due to the different results of evaluation procedures, partly due to the deviations in the α vs. B^2 curves above $B^2 \approx 6 \cdot 10^{-3}$cm^{-2}. One possible - though improbable - explanation might be derived from a recent paper of Ghatak and Honeck /25/. These

authors note that the critical limit for the eigenvalues in graphite as derived from the Parks model is $\approx 1000 sec^{-1}$ instead of the value $\approx 2600 sec^{-1}$ derived from the measured cross section. This may be due to inaccuracies in the Parks model or in the measured cross section. If the latter were true and 1000 sec^{-1} the actual critical limit, no stable asymptotic mode would exist for $B^2 \gtrsim 5 \cdot 10^{-3}$ cm^{-2}, i.e. only the region $0 < B^2 < 5 \cdot 10^{-3}$ cm^{-2} could be used for analysis.

Heavy water

Recent results on D_2O at room temperature are summarized in table 6. It is seen that the measurements are in a reasonable agreement among themselves and that the parameters are well represented by the theoretically predicted parameters. The latter are for pure D_2O and should be slightly decreased which makes the agreement even better. Ganguly, Cobb and Waltner have also reported diffusion parameter measurements in the temperature range 10 - 50° C.

Table 6 Diffusion parameters of D_2O (99 8%) at room temperature

D_o ($cm^2 sec^{-1}$)	C ($cm^4 sec^{-1}$)	Remarks	
$2.00 \pm 0.01 \cdot 10^5$	$5.25 \pm 0.25 \cdot 10^5$	3-par. fit, $1.3 \cdot 10^{-3}$ B^2 $45 \cdot 10^{-3}$ cm^{-2} 22° C	Exp. by Kussmaul and Meister /42/
$2.045 \pm 0.044 \cdot 10^5$	$4.706 \pm 0.381 \cdot 10^5$	3-par. fit[5] $16 \cdot 10^{-3}$ B^2 $85 \cdot 10^{-3} cm^{-2}$ 21° C	Exp. by Malaviya and Profio /43/
$2.039 \pm 0.013 \cdot 10^5$	$4.18 \pm 0.18 \cdot 10^5$	3-par. fit[6] $30 \cdot 10^{-3}$ B^2 $90 \cdot 10^{-3} cm^{-2}$ 28° C	Exp. by Westfall and Waltner /57/
$2.06 \pm 0.05 \cdot 10^5$	$3.72 \pm 0.5 \cdot 10^5$	3-par. fit[6] $60 \cdot 10^{-3}$ B^2 $100 \cdot 10^{-3} cm^{-2}$ 20° C	Exp. by Ganguly, Cobb and Waltner /44/
$2.069 \cdot 10^5$	$4.852 \cdot 10^5$ ... $5.13 \cdot 10^5$	calculation by Honeck /40/ using incoherent scattering model for D_2O	
$2.09 \pm 0.02 \cdot 10^5$	—	calculated by Springer et al. /29/ from $\Sigma_s(E)$ and $\bar{\mu}(E)$ 20° C	

Other moderators

In table 7, some more recent data reported on various other moderators are listed. Many data on measurements published before 1962 are summarized in [45].

Table 7 Diffusion parameters of various moderators

Material	Density	Temperature	$\overline{v\Sigma_a}(sec^{-1})$	$D_o(cm^2sec^{-1})$	$C(cm^4sec^{-1})$	Ref.
Be	$1.79gcm^{-3}$	20^oC	262 ± 11	$1.24\pm0.013 \cdot 10^5$	$3.68\pm0.20 \cdot 10^5$	[14]
BeO	$2.79gcm^{-3}$	20^oC	174 ± 6	$1.56\pm0.01 \cdot 10^5$	$4.12\pm0.27 \cdot 10^5$	[14]
water		0^oC	4740 ± 90	$32,400 \pm1000$	4200 ± 1000	[46]
ice		0^oC	4470 ± 80	$34,600 \pm1000$	8300 ± 2000	[46]
ice	$0.917gcm^{-3}$	-80^oC		$26,600\pm900$	6600 ± 1000	[47]
ice		-196^oC	4656 ± 200	9500 ± 400	2000 ± 1000	

The new Russian experiments on beryllium and on beryllium oxide indicate a much higher amount of diffusion cooling than previous experiments. The Czech data on water and ice at 0^oC are impressive since they reveal the strong effect which the phase transition has on the thermalization power. A similar observation was made by the Russian group.

2.6 Friedman's method.

The most elementary thermalization property of a scattering medium is the inelastic part of the P_o component of its scattering law, i.e. the quantity

$$\sigma_s(E' \to E) = \int_{-1}^{+1} \sigma_s(E' \to E, \cos\vartheta_o)\, d\cos\vartheta_o$$

5) $\alpha_o = 10\ sec^{-1}$ assumed in evaluation of α vs. B^2 curve

6) $\alpha_a = 0$ assumed in evaluation of α vs. B^2 curve

As is well known, the classical pulsed source technique is not the ideal method to measure quantities which depend sensitively on the above $\sigma_s(E' \rightarrow E)$. Rather, α vs. B^2 curves are also strongly dependent on the transport properties of the medium, viz., the elastic scattering angular distribution. Especially the diffusion cooling coefficient is a complicated function of both the transport and the thermalization properties. Early attempts have been made to separate both effects in a simple way, for instance the famous Nelkin /48/ formula

$$C = \frac{D_o^2 \cdot \sqrt{\pi}}{v_o \cdot M_2} \left(p + 1/2 \right)^2 \tag{6}$$

has frequently been used where M_2 is the second moment of the scattering law in an equilibrium Maxwellian,

$$M_2 = \iint \Sigma_s(E' \rightarrow E) \frac{(E' - E)^2}{(kT_o)^2} \frac{E}{kT_o} e^{-E/kT_o} \frac{dE}{kT_o} dE' \tag{7}$$

and p is the exponent in the approximate relationship

$$\lambda_{tr}(E) \sim E^p \tag{8}$$

However, equ. (6) holds only approximately, it depends sensitively on the assumption that $\lambda_{tr}(E)$ can be represented by equ. (8). In order to derive M_2 from a measured C, p must be accurately known. Thus it is difficult to derive direct information on thermalization properties from measured α vs. B^2 curves and people have searched for other suitable methods.

An obvious approach is to measure the decay of a thermalized pulse in an infinite medium which contains a non-1/v absorber. While in the presence of a 1/v absorber or in a non-absorbing medium the asymptotic spectrum is strictly Maxwellian, a non-1/v absorber will deform the asymptotic spectrum. Simply, the spectrum will be "cooler" for σ_a decreasing slower than 1/v and "hotter" for σ_a decreasing faster than 1/v. Whereas the relation between the decay constant α as a function of the absorber concentration N is linear in case of a pure 1/v absorber, it will actually show a downward curvature as a result of the fact that the apparent absorption cross section becomes smaller. This downward curvature will be the stronger the stronger the deviations of $\sigma_a(E)$ from the 1/v law are, it is also greatly influenced by the isotropic part of the thermalization kernel.

Although measurements of this type have been done several times in the past [49, 50], the first author who realized the full possibilities of this approach was Friedman [51 - 53]. He described the α vs. N relationship in an infinite medium by the expression

$$\alpha = \alpha_o + \frac{2v_o}{\sqrt{\pi}} N \left\{ a + b N + ... \right\} \tag{9}$$

where $\alpha_o = (v \Sigma_a(v))_{1/v}$ describes the fixed 1/v absorption of the "solvent". a is the Maxwell averaged absorption cross section of the added absorber,

$$a = \int_o^\infty \left(\frac{E}{kT_o} \right) e^{-E/kT_o} \sigma_a(E) \frac{dE}{kT_o} \tag{10}$$

and the higher coefficients b, c ... depend on the thermalization properties of the solvent and the non-1/v behaviour of $\sigma_a(E)$. Describing the deviations of the asymptotic spectrum $\Phi(E)$ from the equilibrium Maxwellian by means of an expansion into Laguerre polynomials of order unity,

$$\Phi(E) = \frac{E}{(kT_o)^2} e^{-E/kT_o} \sum_k A_k L_k \left(\frac{E}{kT_o} \right) , \tag{11}$$

Friedman could express b (and in principle the higher terms c, d, etc.) in terms of matrix elements

$$\gamma_{ik} = \int_o^\infty L_i \left(\frac{E}{kT_o} \right) H L_k \left(\frac{E}{kT_o} \right) \frac{E}{kT_o} e^{-E/kT_o} \frac{dE}{kT_o} \tag{12}$$

(with H = isotropic thermalization operator) and

$$S_k = \int_o^\infty \left\{ \frac{2}{\sqrt{\pi}} v_o \frac{a}{v} - \sigma_a(E) \right\} L_k \left(\frac{E}{kT_o} \right) \left(\frac{E}{kT_o} \right) e^{-E/kT_o} \frac{dE}{kT_o} \tag{13}$$

Since the S_k are well-known if $\sigma_a(E)$ was carefully measured, b (and c, etc.) can be calculated to an accuracy depending only on the accuracy of the γ_{ik}, i.e. on the isotropic part of the scattering law. Conversely, if b was derived from a fit of the α vs. N curve, information on the γ_{ik} can be obtained. The relation between b and the γ_{ik} and S_k is however complex. If one assumes that the two Laguerre polynomials k = 0 and k = 1 are sufficient in order to describe the disturbed spectrum [7], the relation between b and the γ matrix simply

---

7) This assumption, as is well known, corresponds to the "shifted neutron temperature concept".

becomes

$$b = -\frac{S_1^2}{\gamma_{11}} \qquad (14)$$

and γ_{11} can be immediately derived. As one can easily show, $\gamma_{11} = \frac{1}{4} M_2$ and we thus have a simple method for the determination of the second moment of the scattering kernel.

Experimentally, the method is not as simple as this. The measurements are not performed at infinite geometry. In order to eliminate the effects of diffusion on α, α is determined at each absorber concentration as a function of B^2 and an extrapolation to $B^2 = 0$ is made. Friedman investigated aqueous solutions of Cd, Sm, Gd and Sm-Gd mixtures. He performed measurements in the range $0.096\ cm^{-2} < B^2 < 0.15\ cm^{-2}$. The paramount problem in this type of measurement is the elimination of spatial modes in the rather large vessels filled with strongly absorbing solutions. Unfortunately, no decay curves are shown in his publications. From the measurements on the above mentioned solutions, he derived $M_2 = 0.84 \pm 0.1\ cm^{-1}$ for H_2O using equ. (14). By a similar method, Verdaguer et al. /54/ found $M_2 = 1.46 \pm 0.43\ cm^{-1}$ for water. Both results are much lower than those derived by equ. (6) from "standard" pulsed experiments and which are $\approx 3\ cm^{-1}$. The value calculated on the basis of the Nelkin model is $3.2\ cm^{-1}$. Gläser /55/ has calculated M_2 from the Haywood-Thorson experimental scattering law of water and found $M_2 = 3.1\ cm^{-1}$. Thus there is strong evidence against the M_2 values derived by Friedman's method. There might be an error in the above value due to the use of the approximate equ. (14) instead of the more accurate original equation. However, Calame /56/ has calculated accurate b values on the basis of the Nelkin model, comparing his result with those derived from equ. (14) shows that the approximation is a very good one. The explanation of the discrepancies might be

- errors in the input values of σ_a (E) used for the determination of the S_k. According to Calame, who did some numerical experiments, this is not very probable;

- errors in the α determination due to higher spatial modes;

- errors in the extrapolation to zero buckling.

It would be extremely useful to investigate these questions further since basically this method appears very attractive. The proposal to perform a

spatial Fourier analysis on large D_2O systems /58/ appears to be excellent to meet some of these objectives.

2.7 Buckling determinations by the pulsed technique.

It is well known that once the α vs. B^2 relation is known for a substance, bodies of arbitrary shape can be built from this material and their B^2 be determined by α measurements. Such investigations have been done frequently, but since their results are of a highly specialized nature, not many results have been published in the open literature. The interest mainly lies in the effect of oddly-shaped control elements and in streaming effects caused by holes and voids in homogenous media.

3. Transient Phenomena

3.1 Measurements of the slowing-down time to definite energies.

Depending on the availability of suitable resonance detectors, slowing-down time measurements to definite energies in the epithermal and near-thermal range can be made. Such experiments have been done using In (1.46 eV), Pu (0.3 eV), Cd (0.178 eV) and Sm (0.0976 eV) as a resonance detector; some authors have also used a thick cadmium indicator which has an "edge" in the absorption cross section at 0.5 eV. [8] Resonance capture indication is either "positive", i.e. by observation of capture γ-rays or fissions, or "negative", i.e. by observation of the neutron transmission through the resonance absorber. In any case, a time-dependent reaction rate curve of the type illustrated in Fig. 6 is obtained. There are several ways to derive a slowing-down time from this curve: Most authors consider the time displacement of the maximum as the proper slowing-down time while some authors use the average displacement. Which of the two definitions is used is irrelevant if the proper theoretical value is used in the comparison. Theoretical calculations for the time-energy distribution of neutrons slowed down by free nuclei at rest were performed by Ornstein and Uhlenbeck /60/, Dyad'kin and Batalina /61/ and by Koppel /62/, among others. The ideal experiment is performed by measuring the space-integrated resonance reaction rate in a sufficiently large scattering medium. If localized resonance absorbers are used, the

8) Using the slowing-down time spectrometer, time-dependent capture rates in resonances in the high eV and low keV range have also been observed /59/; this technique is however outside the scope of this review.

results are affected by diffusion times. Corrections for this effect can be made but are difficult to formulate.

The most recent measurements of this type reported are those of Zhezherun et al. /14/. These authors observed the neutron transmission through indium, cadmium and samarium as well as the time-dependent fission rate of a Pu chamber shielded by Sm and Cd. Their experimental results (slowing-down times defined by the displacement of the maximum of the resonance reaction rate curves) are summarized in table 8. Theoretical values for slowing-down by free nuclei at

Table 8 Slowing-down times in Be and Be O /14/

	t(/us) in Be		t (/us) in Be O	
Energy (eV)	Experiment	Theory	Experiment	Theory
1.46	7.5 ± 1	7.2	9.5 ± 1	9.3
0.3	17.5 ± 1	15.7	26 ± 2	19.2
0.178	40 ± 3	20.4	51 ± 3	20.3
0.0976	73 ± 5	27.6	88 ± 5	34.8

rest are shown for comparison and it is seen that while for 1.46 eV the agreement is excellent, this theory underestimates the experimental values the more the lower the resonance energy drops. This is of course a consequence of the thermal motion of the moderator atoms and of their chemical binding which is very strong in Be and Be O.

Some experiments on slowing down to Cd and In energies have been performed recently in H_2O and D_2O. Since slowing down proceeds very fast in these moderators, especially in H_2O, the experiments are difficult to perform and require a high timing accuracy for the source burst and the neutron detection equipment. Results of Profio and Eckard /63/ are shown in table 9. Slowing-down times were defined by the displacement of the maximum. It is seen that agreement between measured and calculated values is good except the Cd/D_2O value. This difference is attributed to diffusion time effects (which were not corrected for) rather than to effects of chemical binding or thermal motion. Möller and Sjöstrand /64/ found independently that chemical binding and thermal motion play no important role in the slowing-down to the cadmium edge in H_2O.

Table 9 Slowing-down times in H_2O and D_2O [63]

	t(μsec) measured		t(μsec) calculated	
	In resonance	Cd edge	In resonance	Cd edge
H_2O	0.75 ± 0.5	1.75 ± 0.5	0.6	1.65
D_2O	4.0 ± 1.0	10.5 ± 1.0	4	8

Profio and Eckard have suggested to use time-dependent reaction rate measurements in moderating assemblies as a more general tool for reactor physics studies. For instance, they suggest to determine resonance capture probabilities in this way and to separate the thermal and epithermal activation of flux indicators from the time dependency. No work of this type has been published so far.

3.2 Investigation of time-dependent neutron thermalization

The most powerful tool for investigating the time-dependent neutron thermalization is the detailed measurement of the time-dependent spectrum using a pulsed source and synchronized chopper. This method necessitates very strong neutron sources and a time-of-flight spectrometer and does not belong to the class of simple pulsed source experiments reviewed in this paper [9]. Considerably simpler - though less informative - are measurements of the approach to equilibrium of certain spectral indices after the injection of a fast source burst. Three different kinds of spectral indices have been in use, viz.,

- the average neutron velocity, as determined by the counting rate ratio between a thick (black) and a thin (1/v) BF_3 counter;
- the average cross section of non-1/v absorbers like Cd and Gd as measured by the intensity of capture γ-rays;
- the effective cross section of 1/v absorbers as determined by a transmission experiment.

[9] Cf. the review article of M.J. Poole [65]

The interpretation of these time-dependent spectral indices is difficult. Early workers have assumed that the spectrum at any time could be described by a Maxwellian and have derived a time-dependent neutron temperature T(t) from their measured spectral indices. Using the elementary relation

$$T(t) - T(t=\infty) \sim e^{-t/t_{th}} \qquad (15)$$

values of a "thermalization time" t_{th} were deduced. Later on, it became evident that the effective temperature concept was inappropriate since the spectra deviate greatly from pure maxwell distribution, especially in moderators with strong chemical binding. Then, the "energy mode concept" was introduced in which it is assumed that the time-dependent spectrum $\Phi(E,t)$ can be represented by a superposition of separate modes, viz.,

$$\Phi(E,t) = \Phi_{as}(E) \cdot e^{-\alpha t} + \Phi_1(E)\, e^{-\lambda_1 t} + \Phi_2(E)\, e^{-\lambda_2 t} + \ldots. \qquad (16)$$

α is the fundamental mode decay constant which is usually observed in pulsed source experiments whereas the higher modes characterize the transients during the thermalization process. The $\lambda_{1,2\ldots}$ are dependent on the thermalization power of the moderator and in particular λ_1 is considered to be a characteristic quantity. $1/\lambda_1$ is sometimes called "thermalization time constant". If the fundamental mode decay constant α is known, the contribution of the fundamental mode to a time-dependent spectral index can be "peeled off" and λ_1 can be determined. This evaluation, however, presupposes that a representation of the time-dependent spectrum by separate modes is possible. Unfortunately, theory has recently shown [25, 66] that in most crystalline moderators, especially in graphite and beryllium, no such representation is possible. In these media, the fundamental mode decay constant is the only discrete eigenvalue below the critical limit - and even that only at sufficiently small bucklings as repeatedly stated - whilst all other eigensolutions belong to the continuum which extends above the critical limit, none of these can be isolated. Fortunately, in H_2O at least λ_1 and λ_2 are predicted to be discrete.

The experimental results reflect the difficulties in the evaluation procedure. In water, Möller and Sjöstrand [64, 67] were able to isolate the first energy mode by reaction rate measurements on Cd and Gd, they found $\frac{1}{\lambda_1} \approx 4$ µsec for a

large geometry. Theoretically, on the basis of the Nelkin model $\frac{1}{\lambda_1} = 5.4$ /usec is predicted /66/ which agrees remarkably well. In graphite, several new results exist which are discrepant: Serdula /12/ determined time-dependent neutron temperatures by neutron transmission through silver absorbers. He interpreted his data according to equ. (15) and determined t_{th} as a function of B^2 in the range $4 < B^2 < 14.5 \cdot 10^{-3}$ cm^{-2}. Extrapolating to $B^2 = 0$, $t_{tn} = 750 \pm 200$ /usec was found. Küchle and Schweikert /68/ performed transmission measurements through silver absorbers and analysed their data according to equ. (16). Their values of λ_1 vs. B^2 are shown in Fig. 7; note that some of them are > 2600 sec^{-1}. Extrapolating to $B^2 = 0$, $\frac{1}{\lambda_1} = 550 \pm 50$ /usec was found. Starr, Honeck and de Villiers /41/ measured the average neutron velocity as a function of time for graphite stacks in the buckling range $1.77 \ldots 15.05 \cdot 10^{-3}$ cm^{-2}. Although the main purpose of their experiment was the determination of the asymptotic average velocity, they tried to derive information on the speed of the thermalization process. It was found that the average velocity approaches its asymptotic value nearly exponential with a time constant of about 525 /usec which was found to be quite independent of B^2. In view of the large discrepancies of these various results and furthermore in view of the fact that no clear definition of the thermalization time can be given at present, the problem of time-dependent thermalization in graphite must be considered as still largely unsolved. The only conclusion which can be drawn from more recent studies is that the time scale of the thermalization process in graphite is about 2 to 3 times slower than observed in the very first studies. The reasons for this have been previously discussed /69/.

In the framework of their very careful work on diffusion and slowing-down in Be and Be O, Zhezherun et al. /14/ have determined time-dependent neutron temperatures by the transmission method. Using equ. (15) and extrapolating to infinite geometry, $t_{th} = 185 \pm 20$ /usec (Be) and $t_{th} = 204 \pm 20$ /usec (BeO) was found. No detailed theoretical analysis of these values - which are higher than previously determined t_{th} figures - has been performed so far.

4. Pulsed Neutron Studies in the Fast Neutron Range

In view of the increasing interest in fast reactor physics and with the availability of intense nanosecond-bunched fast neutron generators, some groups have lately started to apply the pulsed technique to the study of neutron diffusion and moderation in the keV and MeV range. There are several possibili-

ties in this field, for instance measurements of the time-dependency of inelastic moderation, time-of-flight measurements of the neutron spectrum or studies of monoenergetic neutron diffusion. We shall restrict ourselves to the latter application.

The pioneer work in this field was done by Beghian and his collaborators at MIT [70, 71]. This group studied the time decay of monoenergetic neutron fields (energy range 0.8 - 1.6 MeV) in assemblies of iron, bismuth, lead and in natural uranium. Apart of iron which will be discussed below, these are very heavy materials and the slowing-down by elastic collision can be neglected at least to a good approximation. If inelastic scattering is disregarded for the moment, the time-dependency of the diffusion of a burst of fast monoenergetic neutrons can be described by usual one-group theory. After decay of spatial harmonics, the neutron field will therefore die away exponentially with time and the decay constant will be given by

$$\alpha = v\Sigma_r + D_o B^2 + C_T B^4 \qquad (17)$$

where Σ_r and D_o are the removal cross section (see below) and the diffusion coefficient, evaluated at the proper energy. C_T is the well-known transport theory correction to elementary diffusion theory,

$$C_T = \frac{v}{45\,\Sigma_t^3} \qquad (18)$$

for isotropic scattering according to Sjöstrand [72].

The experimental arrangement used by Beghian et al. is shown in Fig. 8. Monoenergetic neutrons were produced by bombarding ≈ 50 keV thick lithium targets with monoenergetic protons from a pulsed van de Graaff generator. Neutrons emerging from the assemblies were detected by a 1" x 1" plastic scintillation counter. This was biased in such a way that neutrons which had undergone an inelastic scattering process and thus had lost an appreciable amount of energy were not detected. Σ_r as defined by equ. (17) thus represents removal processes, i.e. absorption as well as inelastic scattering, and is essentially equal to the nonelastic cross section [10] usually determined by spherical shell transmission measurements. A typical decay curve for a lead

10) Since the biased scintillation detector is not an ideal threshold detector, there remains an appreciable detection probability for neutrons which have been inelastically scattered forming low-lying excited states. For instance, scattering processes leading to the 44 keV 2^+ level in U 238 are not registered as removals and the measured Σ_r must be interpreted accordingly.

block 8 x 8 x 8 inch^3 at 1.24 MeV is shown in Fig. 9 and it is seen that the decay is nearly exponential, allowing a value of α to be derived. An α vs. B^2 curve in uranium at E = 0.84 MeV is shown in Fig. 10. The full curve is a least squares fit according to equ. (17). Since three experimental points are not sufficient to determine three parameters, a calculated value of D_o derived from scattering data of U 238 was used. From this evaluation, $\sigma_r = 0.76 \pm 0.08$ barn was obtained; this is roughly consistant with $\sigma_r = 0.6 \pm 0.14$ which is obtained by adding up $\sigma_{n,\gamma}$ and the inelastic cross sections for the excitation of the 700 keV and (partly) for the 150 keV level. Similar results were obtained for lead.

In the case of iron the elastic moderation cannot be neglected (A = 56). This has two consequences on the observed neutron decay: First, due to the decreasing neutron velocity, the decay of the neutron density will not be strictly exponential. Rather, the decay constant will slowly decrease with time (since the $D_o B^2$ term normally represents the main contribution to α). This effect was considered to be negligible by Beghian et al. Secondly, since the sensitivity of the neutron detector decreases markedly with the neutron energy, the counting rate will decrease faster than the neutron density. Beghian et al. were able to show that this effect can be described by introducing an additional "effective elastic removal cross section" term, $\Sigma_p = \frac{b \cdot \overline{\Delta E}}{\lambda_{tr}}$, into equ. (17). Here $\overline{\Delta E}$ is the average energy loss in an elastic collision, λ_{tr} is the transport mean free path and b is a constant characteristic for the shape of the detectors' energy-dependent efficiency curve. Correcting the measured data in this way, the measured removal cross sections were found to agree with other measurements.

Recently, Miessner at Karlsruhe has started similar experiments in the low kilovolt range. The objectives of his work are to measure capture cross sections and to investigate the effect of the cross section resonance structure on integral neutron behaviour. The first of these objectives was mainly initiated by the lack of reliable methods to measure keV capture cross sections absolutely. In these experiments, monoenergetic neutrons at energies below the threshold for inelastic scattering are injected into assemblies of heavy absorbers like uranium, tantalum, antimony or gold. The experimental setup is similar to the one shown in Fig. 8. The $Li^7(p,n)Be^7$ reaction under 0^o at threshold (E = 30 keV) has been used so far but some feasibility studies using the $Sc^{45}(p,n)\ Ti^{45}$ reaction at threshold (E = 5.5 keV) have been performed. The detector is a

Li^6 loaded glass scintillator; it has a very high sensitivity for γ-rays and thus a rather poor signal-to-noise ratio, no better solution has been found so far. A decay curve observed in lead which was used as a test case is shown in Fig. 11.

A closer inspection of the dacay curve after background correction shows that it is not exponential. This is due to the effect of elastic moderation which becomes appreciable after a sufficiently long time. In the particular example shown in Fig. 11, the decay was observed up to 800 nsec after the pulse injection. A neutron of ≈ 30 keV undergoes about 60 collisions during this time interval in lead, whereby its average velocity will decrease by about 35%. Of the two resulting effects on the observed decay mentioned above, the first one - i.e. the reduction of the decay rate - is considered to be the more important one[11]. Since elastic moderation at kilovolt energies is a rather transparent process, it is fairly simple to correct the measured time decay in order to account for elastic moderation. In /73/, a correction factor F(t) is calculated which yields

$$\frac{n_{obs}(t)}{F(t)} \sim e^{-\alpha t} \qquad (19)$$

F(t) depends on the scattering and absorption cross sections of the medium which must be known at least to first order. Arai has written an on-line computer programme to calculate this factor and to correct measured data immediately. It is seen in Fig. 11 that after this correction the measured densities die away exponentially.

Fig. 12 shows a preliminary α vs. B^2 curve which was observed in this way on U 238 [12]. No upward curvature as in the work of Beghian et al. is observed here; this is due to the fact that Σ_t is much larger in the keV than in the MeV region. The slope of the straight line yields $D_o \approx 9.1 \cdot 10^7$ cm^2 sec^{-1} which is much smaller than what would be expected on the basis of the known total cross section. The reason for this discrepancy is unclear at present. The extrapolation to zero buckling yields $\sigma_a \approx 0.44$ barn in rough agreement with what might be expected on the basis of the known uranium cross sections.

---

11) This is so because the $Li^6(n,\alpha)H^3$ cross section is assumed to be still nearly 1/v in this energy range.

12) Actually, the experiment was performed on natural uranium, but the effect of U 235 is considered to be negligible.

In analysing these experiments, the resonance structure of the cross sections must be taken into account. The treatment is considerably simplified by the fact that in the range of energies and mass numbers considered here, the widths of the individual resonances are small as compared to the average energy loss in an elastic collision. Therefore, simple approximations can be used. Under certain simplifying assumptions, the following relations /73/ can be derived for the diffusion parameters:

$$\Sigma_a = f_c \cdot \langle \Sigma_a \rangle \tag{20}$$

$$D_o^{13)} = \frac{v}{3} \cdot \frac{1}{f_t \langle \Sigma_t \rangle} \tag{21}$$

Here, the square brackets mean averaging over an energy interval which is large enough to contain many resonances, but small enough so the average values do not change appreciably. $\langle \Sigma_a \rangle$ and $\langle \Sigma_t \rangle$ are "infinite dilution" average values of the type listed normally in cross section tables. f_c and f_t are the self-shielding factors as defined by Abagjan et al. /74/, viz.,

$$f_c = \frac{1}{\langle \sigma_a \rangle} \cdot \frac{\left\langle \frac{\sigma_a}{\sigma_t} \right\rangle}{\left\langle \frac{1}{\sigma_t} \right\rangle} \tag{22}$$

$$f_t = \frac{1}{\langle \sigma_t \rangle} \cdot \frac{\left\langle \frac{1}{\sigma_t} \right\rangle}{\left\langle \frac{1}{\sigma_t^2} \right\rangle} \tag{23}$$

Values of f_t and f_c are tabulated for many nuclides in /74/.

For U 238 at 30 keV, f_t and f_c are very close to 1 and the self-shielding effects are easily eliminated. In going to lower energies, the self-shielding factors however decrease considerably; at 5 keV, for instance, $f_c \approx 0.55$ and $f_t \approx 0.7$ for U 238. Since at these low energies $\langle \Sigma_a \rangle$ and $\langle \Sigma_t \rangle$ can be accurately determined by other methods, pulsed source methods might be able to determine self-shielding factors in a rather straightforward manner.

13) Isotropic scattering in the laboratory system was assumed here.

5. Summary and Conclusions

It has been shown that although a considerable amount of work on the asymptotic decay of thermalized neutron fields has been done, some of the basic problems still seem to be unsolved. This concerns the question of the decay constant in small crystalline media, the shape dependency of B^2 in small water systems, and the analysis technique for α vs. B^2 curves. In some regions, good progress has been made. So in many cases there is agreement between different measurements on liquid moderators and in H_2O the accuracy of the experiments - which are, however, largely poisoning experiments of the stationary type - is sufficient to permit very detailed comparisons with theory. Friedman's method has been shown to be a very useful tool, there are however large discrepancies between theory and experiment which represent a challenge to experimenters.

Slowing-down time measurements above 0.5 eV are now available for a few moderators and generally corroborate the elementary theory for slowing-down by free nuclei at rest. Thermalization time measurements in water seem to be in a good state while measurements in graphite suffer from the fact that no reasonable definition of a thermalization time is presently offered from theoreticians.

The new field of quasi-asymptotic decay of fast monoenergetic neutron fields deserves further attention. Much more developments in the theory and in the techniques of these experiments are required. In view of the steadily improving techniques for fast neutron differential cross section measurements, it is somewhat doubtful if the pulsed technique will result in substantial improvements of fast reactor data. Rather, it will contribute to a better understanding of the behaviour of fast neutrons in matter.

References

/1/ Corngold, N., this conference, paper SM 62/79.

/2/ Corngold, N. (ed.), Proceedings of the Brookhaven Conference on Neutron Thermalization, BNL 719 (1962), especially Volume III: Experimental Aspects of Transient and Asymptotic Phenomena.

/3/ Corngold, N., Nucl. Sci. Eng. 19 (1964) 80.

/4/ Silver, E., ORNL-3499 (1963) 33.

/5/ Ogrzewalski, Z., et al., Nukleonika VIII (1963) 595.

/6/ Corngold, N., private communication.

/7/ Fullwood, R.R., Slovacek, R.E., and Gaerttner, E.R., Nucl. Sci. Eng. 18 (1964) 137.

/8/ Küchle, M., unpublished.

/9/ Starr, E. and Price, G.A., BNL 719, Vol. III (1962) 1034.

/10/ Klose, H., Küchle, M., and Reichardt, W., BNL 719, Vol. III (1962) 935.

/11/ Sagot, M. and Tellier, H., CEA 2210 (1962); cf. also J. of Nucl. Energy A/B 17 (1963) 347.

/12/ Serdula, K.J., Ph.D. Thesis, Birmingham 1963.

/13/ Davis, S.K., de Juren, J.A., and Reier, M., submitted for publication in Nucl. Sci. Eng.

/14/ Zhezherun, I.F., et al., 3rd ICPUAE 1964, P/362a.

/15/ Küchle, M., Nukleonik 2 (1960) 131.

/16/ Lopez, W.M. and Beyster, J.R., Nucl. Sci. Eng. 12 (1962) 190.

/17/ Hall, R.S., Scott, A., and Walker, J., Proc. Phys. Soc. 79 (1962) 257.

/18/ Brown, J.C.B., Ph.D. Thesis, Birmingham 1963.

/19/ Gelhard, E.M. and Davis, J.A., Nucl. Sci. Eng. 13 (1962) 237.

/20/ Kladnik, R., Nukleonik 6 (1964) 147.

/21/ Judge, F.D. and Daitch, P.B., Nucl. Sci. Eng. 20 (1964) 428.

/22/ Starr, E. and Koppel, J.U., BNL 719, Vol. III (1962) 1012.

/23/ Arai, E. and Küchle, M., submitted for publication in Nukleonik.

/24/ Joest, K.H. and Memmert, G., 3rd ICPUAE 1964, P/762.

/25/ Ghatak, A.K. and Honeck, H., Nucl. Sci. Eng. 21 (1965) 227.

/26/ Clendenin, W.W., Nucl. Sci. Eng. 18 (1964) 351.

/27/ Kallfelz, J., unpublished internal Karlsruhe report, 1965.

/28/ Koppel, J.U. and Young, J.A., Nucl. Sci. Eng. 19 (1964) 412.

/29/ Springer, T., et al., 3rd ICPUAE 1964, P/763.

/30/ Pál, L., et al., 3rd ICPUAE 1964, P/651.

/31/ Küchle, M., and Kussmaul, G., Nukleonik 6 (1964) 329.

/32/ Bayer, R., Červená, J., and Schäferlingová, W., Czech, J. Phys. B 12 (1962) 107.

/33/ Ádám, A., Bod, L., and Pál, L., Acta Phys. Hung. XIII (1961) 25.

/34/ Gläser, W., Nukleonik 7 (1965) 64.

/35/ Yurova, L.N., et al., 3rd IPUAE 1964, P/356.

/36/ Blackshaw, G.L. and Waltner, A.W., J. of Nucl. Energy A/B 17 (1963) 341.

/37/ Charles, M.P., J. of Nucl. Energy 18 (1964) 305.

/38/ Nilsson, T. and Sjöstrand, N.G., Arkiv Fysik 24 (1963) 543.

/39/ Murgatroyd, W., et al., 3rd ICPUAE 1964, P/564.

/40/ Honeck, H., BNL 719 Vol. IV (1962) 1186.

/41/ Starr, E., Honeck, H., and de Villiers, J., Nucl. Sci. Eng. 18 (1964) 230.

/42/ Kussmaul, G. and Meister, H., J. Nucl. Energy A/B 17 (1963) 411.

/43/ Malaviya, B.K. and Profio, A.E., Trans. Am. Nucl. Soc. 1 (1963) 58.

/44/ Ganguly, N.K., Cobb, F.C., and Waltner, A.W., Nucl. Sci. Eng. 17 (1963) 223.

/45/ Beckurts, K.H. and Wirtz, K., in Neutron Physics, Springer-Verlag, Berlin-Göttingen-Heidelberg-New York (1964).

/46/ Dlouhý, Z. and Kvitek, J., J. Nucl. Energy A/B 16 (1962) 376.

/47/ Antonov, A.V., et al., Atomnaya Energiya 12 (1962) 1,22.

/48/ Nelkin, M., J. Nucl. Energy A 8 (1958) 48.

/49/ Santandrea, E., Toselli, F. and Viano, G., 2nd ICPUAE 1958, P/1372.

/50/ Meadows, J.W. and Whalen, J.F., Nucl. Sci. Eng. 9 (1961) 132.

/51/ Friedman, E., Nucl. Sci. Eng. 14 (1962) 420.

/52/ Friedman, E., 3rd ICPUAE 1964, P/509.

/53/ Friedman, E., Nucl. Sci. Eng. 19 (1964) 203.

/54/ Verdaguer, F., et al., 3rd ICPUAE 1964, P/678.

/55/ Gläser, W. and Beckurts, K.H., Nucl. Sci. Eng. 20 (1964) 235.

/56/ Calame, G.P., Nucl. Sci. Eng. 20 (1964) 352.

/57/ Westfall, F.R. and Waltner, A.W., Trans. Am. Nucl. Soc. 5 (1962) 386.

/58/ Döllgast, T., Federighi, F.D., and Zumbrunn, K., this conference, Paper SM 62/91.

/59/ Cf., for instance, Bergman, A.A., et al., 1 st ICPUAE 1964, P/642.

/60/ Ornstein, L.S. and Uhlenbeck, G.E., Physica 4 (1957) 478.

/61/ Dyad'kin, G. and Batalina, E.P., Atomnaya Energiya 10 (1961) 5.

/62/ Koppel, J.U., Nucl. Sci. Eng. 8 (1960) 157.

/63/ Profio, A.E. and Eckard, J.D., Nucl. Sci. Eng. 19 (1964) 321.

/64/ Möller, E. and Sjöstrand, N.G., AB Atomenergie Report RFX-248 (1963).

/65/ Poole, M.J., this conference, Paper SM 62/90.

/66/ Shapiro, C.S. and Corngold, N., submitted for publication in "Physical Review".

/67/ Möller, E. and Sjöstrand, N.G., BNL 719 Vol. III (1962) 966.

/68/ Küchle, M. and Schweickert, E., unpublished.

/69/ Beckurts, K.H., BNL 719 Vol. III (1962) RE 1.

/70/ Beghian, L.E., et al., Nucl. Sci. Eng. 15 (1963) 375.

/71/ Beghian, L.E., et al., Nucl. Sci. Eng. 17 (1963) 82.

/72/ Sjöstrand, N.G., Arkiv Fysik 15 (1959) 147.

/73/ Beckurts, K.H., unpublished internal Karlsruhe report (1964).

/74/ Abagjan, L.P., et al., INDSWG 17 (1963).

Figure Captions

Fig. 1 Neutron die away in beryllium and in a test assembly of polyethylene selected to give approximately the same decay time (from /7/).

Fig. 2 Time after neutron pulse required for the attainment of an asymptotic spectrum as a function of buckling (from /12/).

Fig. 3 The enlarged α vs. B^2 curve for H_2O.

Fig. 4 Experimental arrangement of Arai and Küchle for measurement of diffusion length in a time-dependent neutron field in H_2O.

Fig. 5 α vs. B^2 curves observed in graphite
□ : Starr and Price /9/ 0 : Davis, de Juren and Reier /13/

Fig. 6 Neutron flux distribution at 0.3 eV as a function of time in beryllium as observed with a Sm-Cd shielded Pu fission chamber (from /14/).

Fig. 7 The first higher eigenvalue λ_1 in graphite as a function of geometrical buckling. Note that the two largest values of λ_1 are above the "critical limit".

Fig. 8 Experimental setup used by Beghian et al. /71/ for fast neutron flux decay studies on iron.

Fig. 9 Decay of 1.24 MeV neutron flux in lead as observed by Beghian et al. /71/.

Fig. 10 α vs. B^2 curve in U 238 at 0.84 MeV (Beghian et al. /71/).

Fig. 11 Decay of 30 keV neutron field in a 15 x 20 x 30 cm^3 lead block.

Fig. 12 α vs. B^2 curve for 30 keV neutrons in natural uranium.

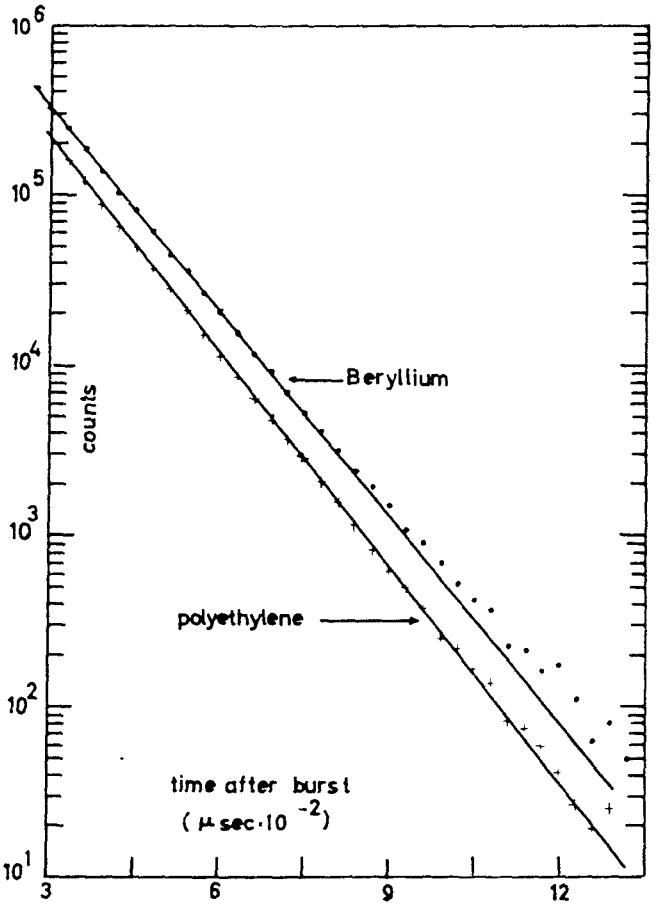

Fig.1. Neutron die–away in beryllium and in a test assembly of polyethylene selected to give approximately the same decay time (from [7])

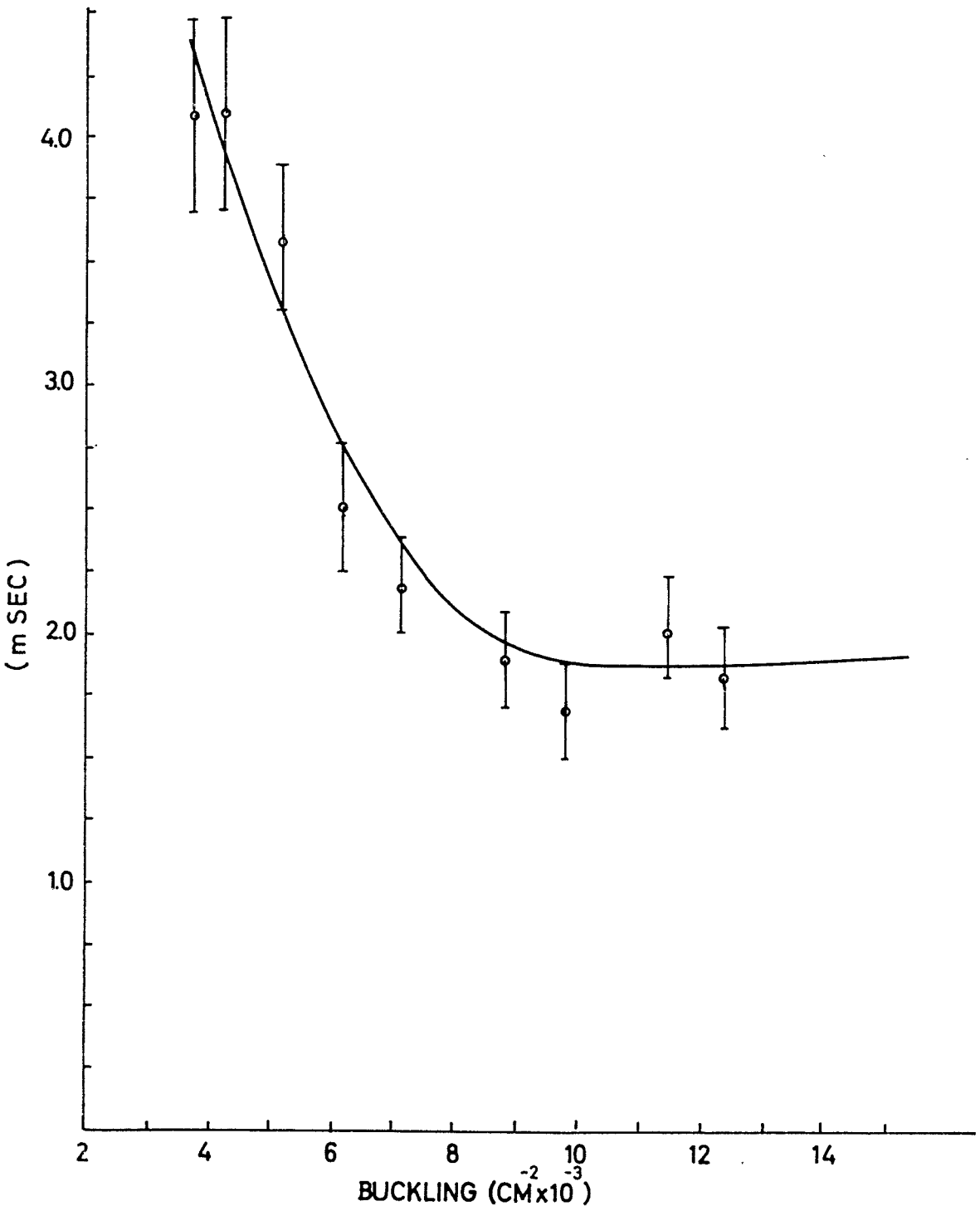

Fig.2. Time after neutron pulse required for the attainment of an asymptotic spectrum as a function of buckling.(from[12]).

Fig. 3 The enlarged α vs. B^2 curve for H_2O

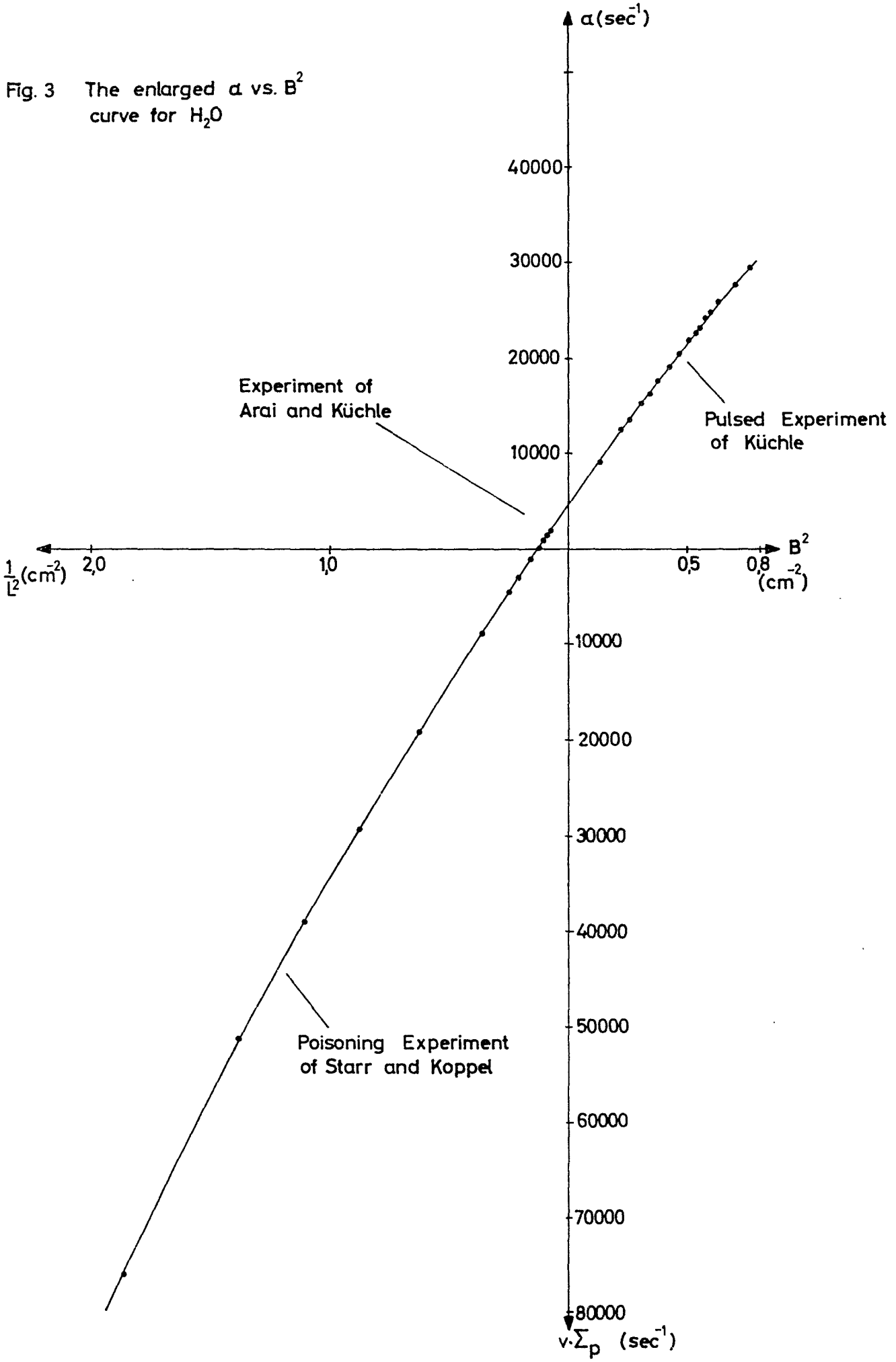

Fig.4 Experimental arrangement of Arai and Küchle for measurement of diffusion length in a time-dependent neutron field in H_2O

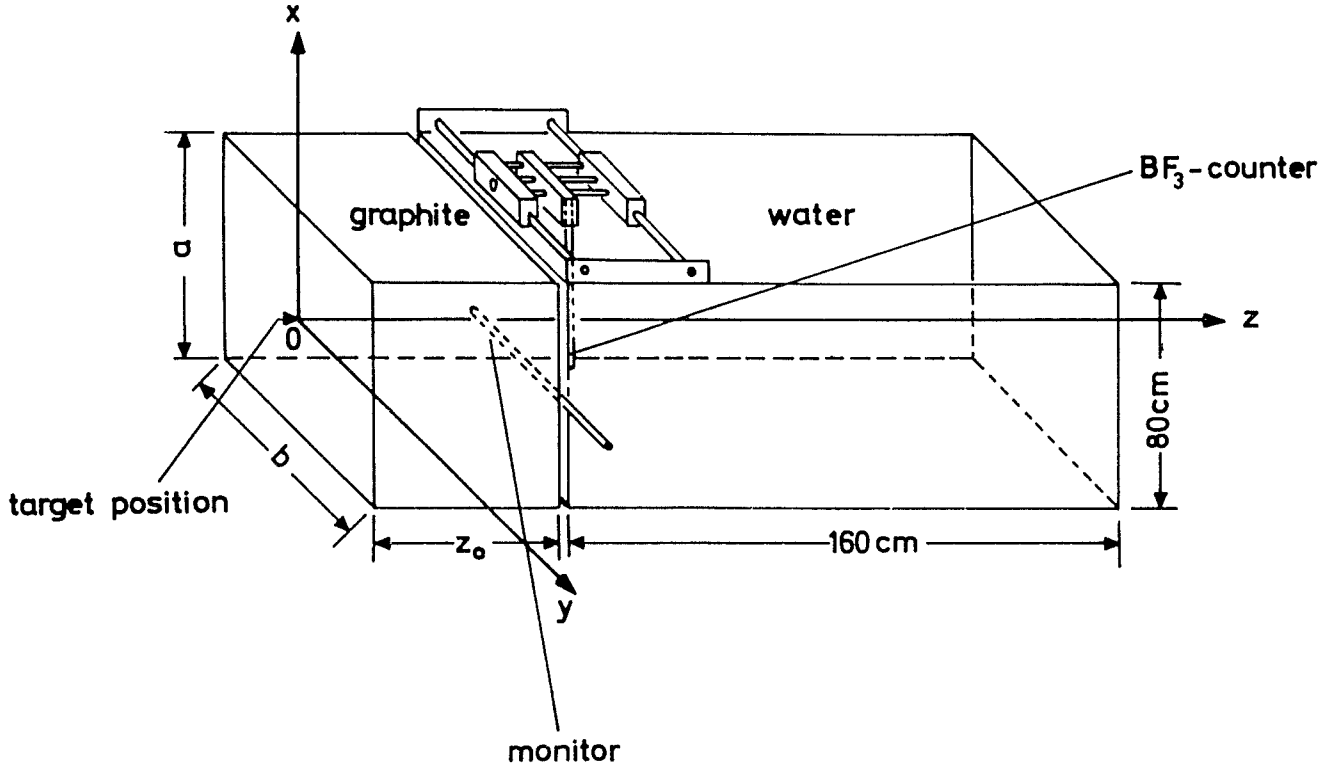

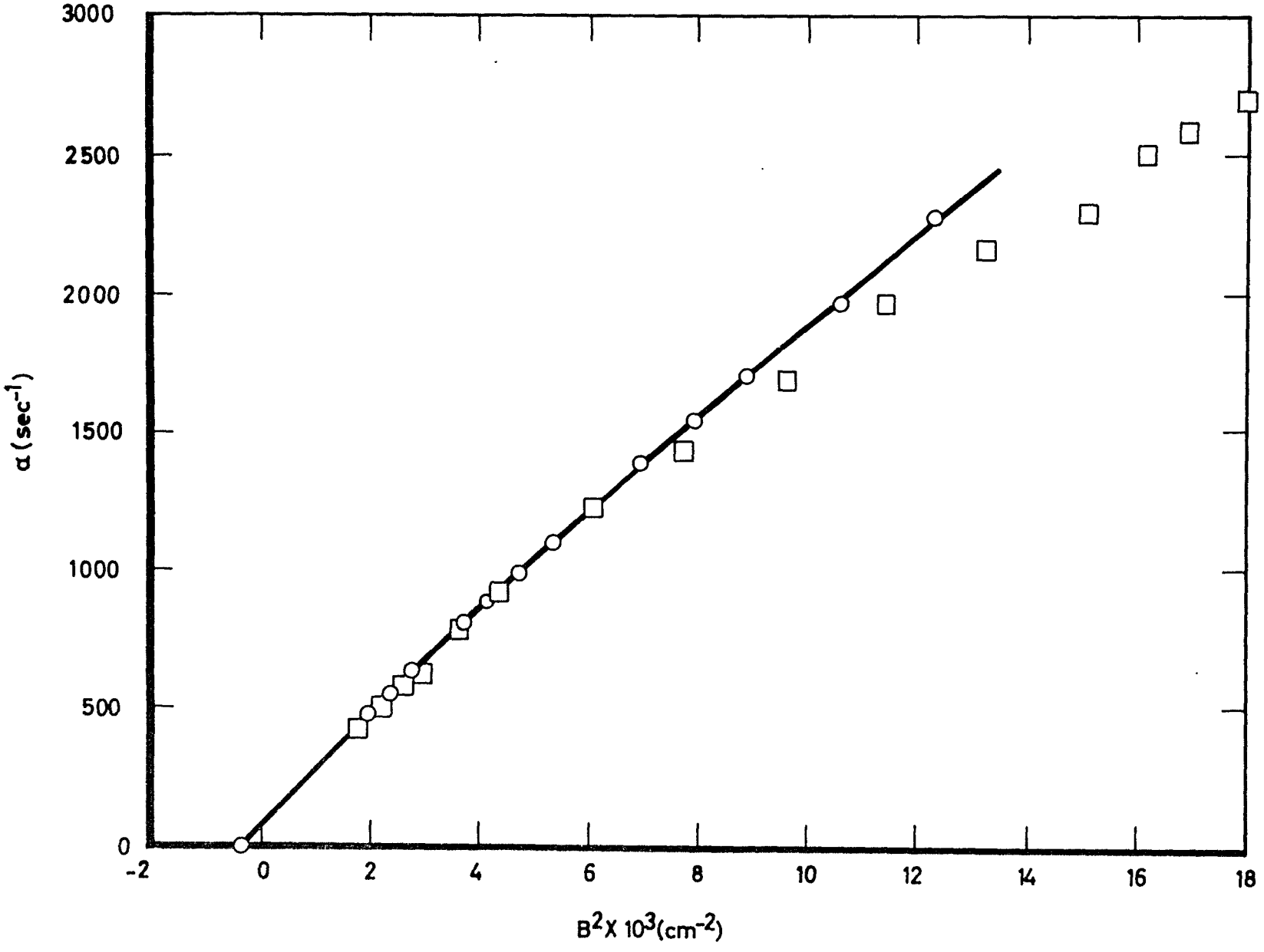

Fig.5 α vs. B^2 curves observed in graphite
□ : Starr and Price [9] O: Davis, de Juren and Reier [13]

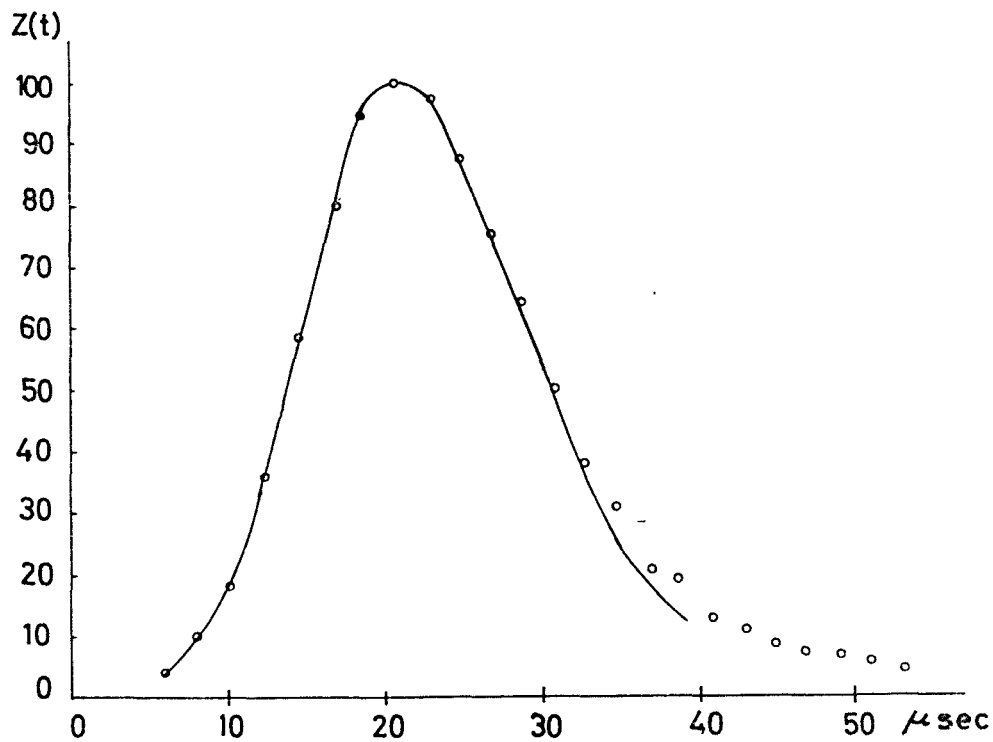

Fig.6 Neutron flux distribution at 0.3 eV as a function of time in beryllium as observed with a Sm-Cd shielded Pu fission chamber (from [14]).

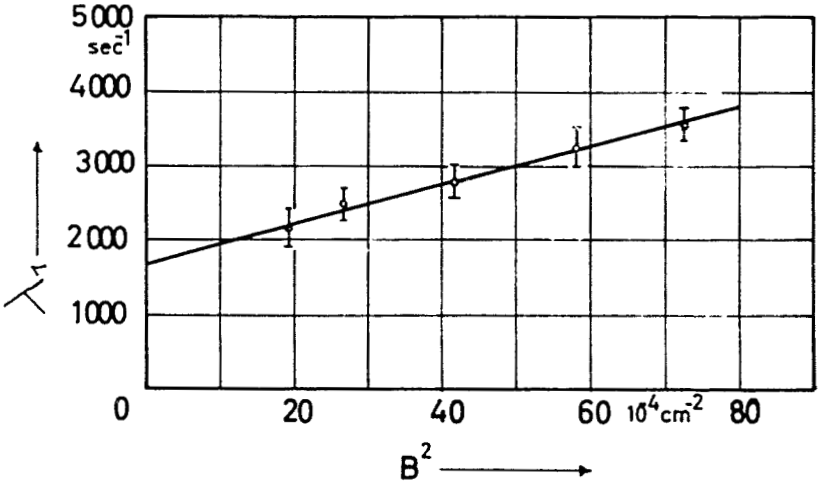

Fig.7. The first higher eigenvalue λ_1 in graphite as a function of geometrical buckling. Note that the two largest values of λ_1 are above the "critical limit".

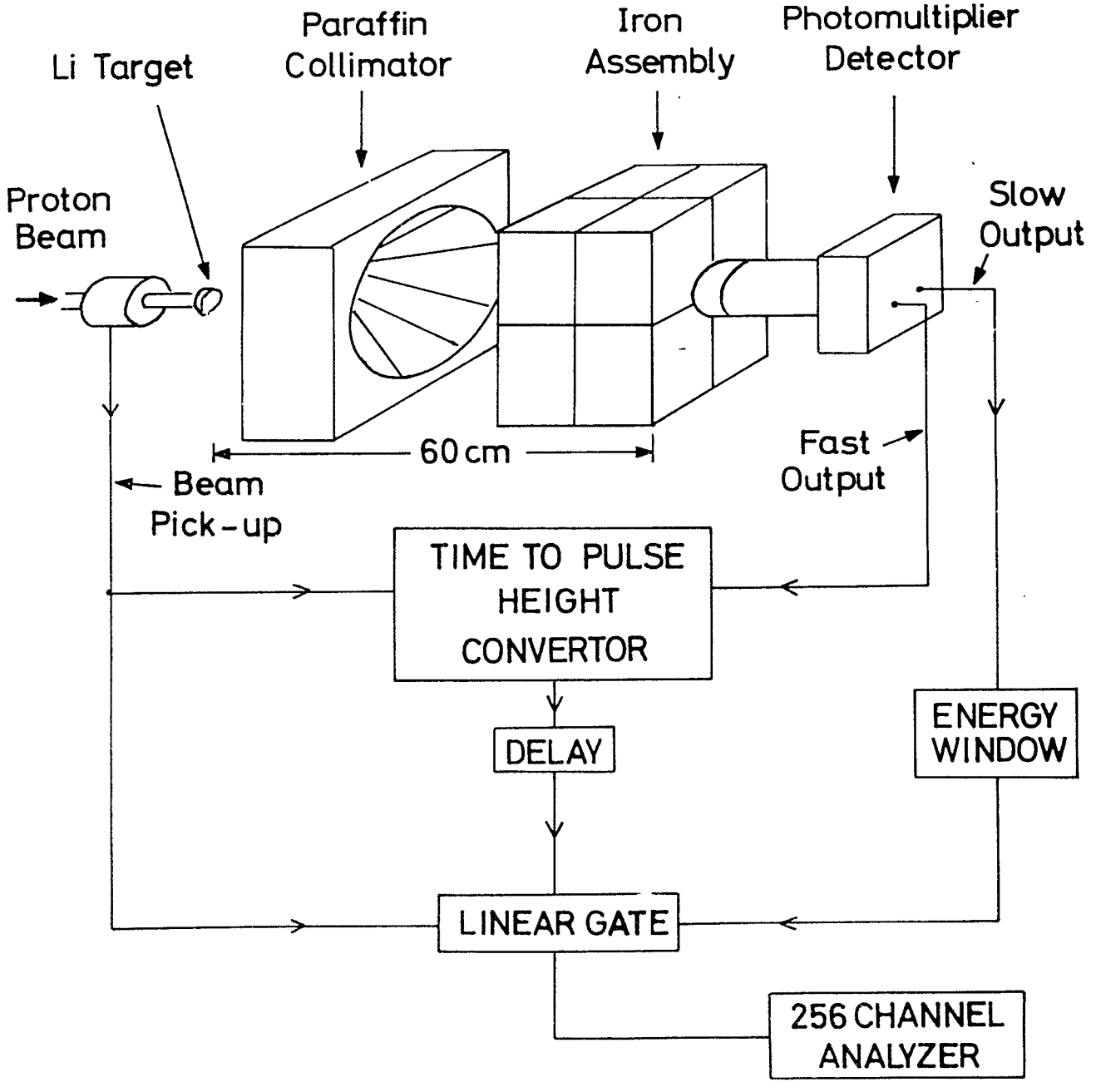

Fig. 8 Experimental setup used by Beghian et al [71] for fast neutron flux decay studies on iron

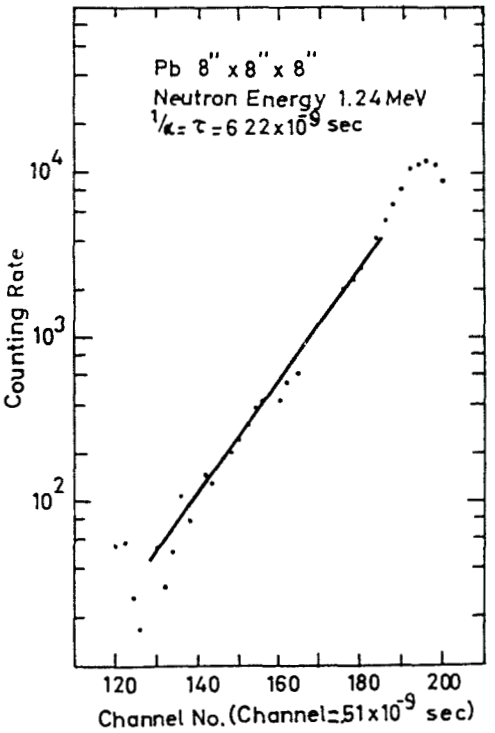

Fig 9 Decay of 1.24 MeV Neutron Flux in lead as observed by Beghian et al.[71]

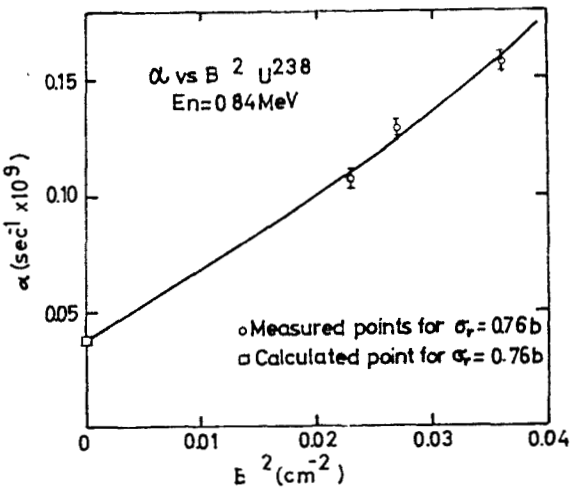

Fig.10 α vs B^2 curve in U^{238} at 0.84 MeV
(Beghian et al.[71])

Fig. 11. Decay of 30 KeV neutron field in a 15x20x30 cm^3 lead block.

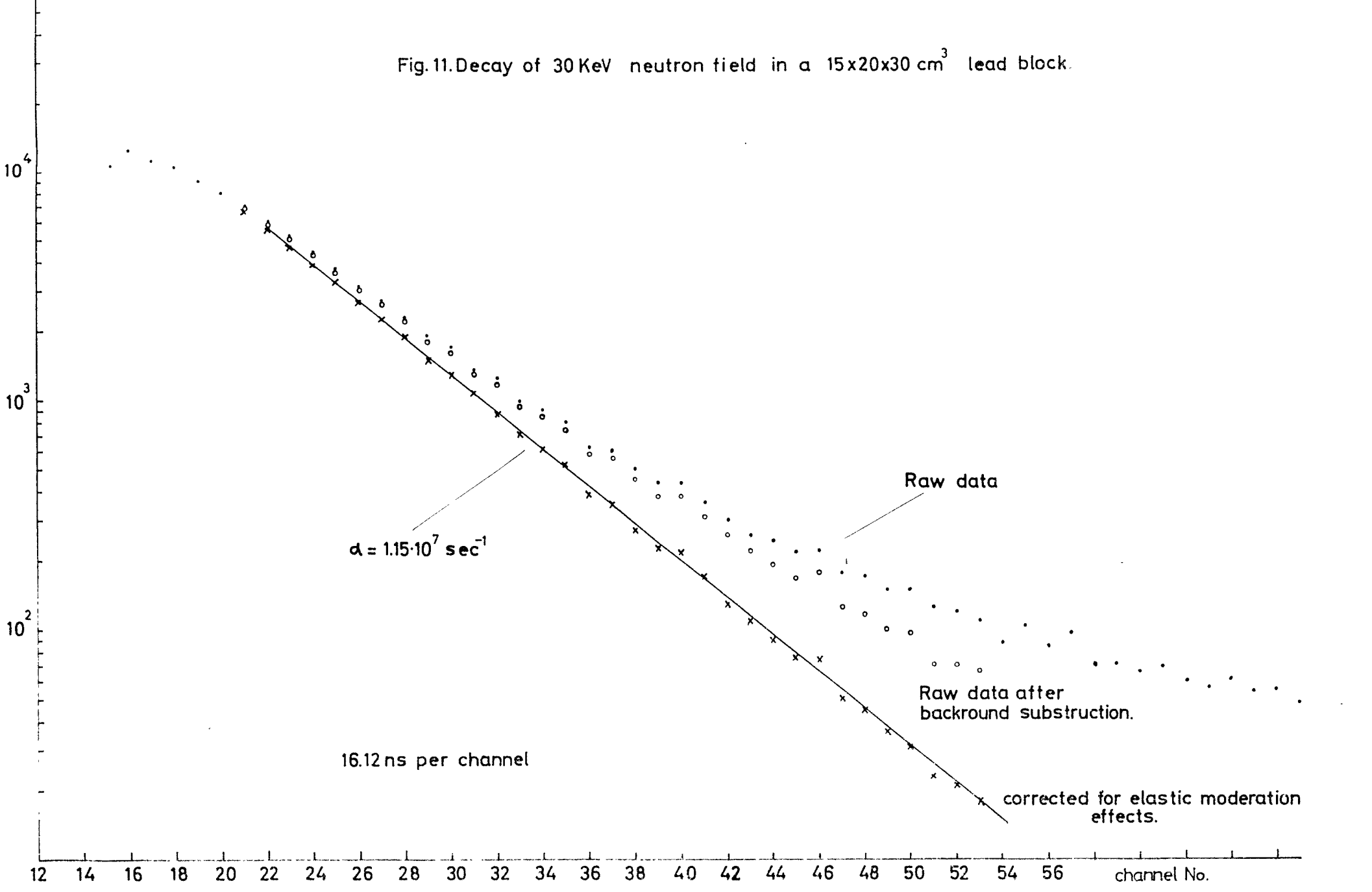

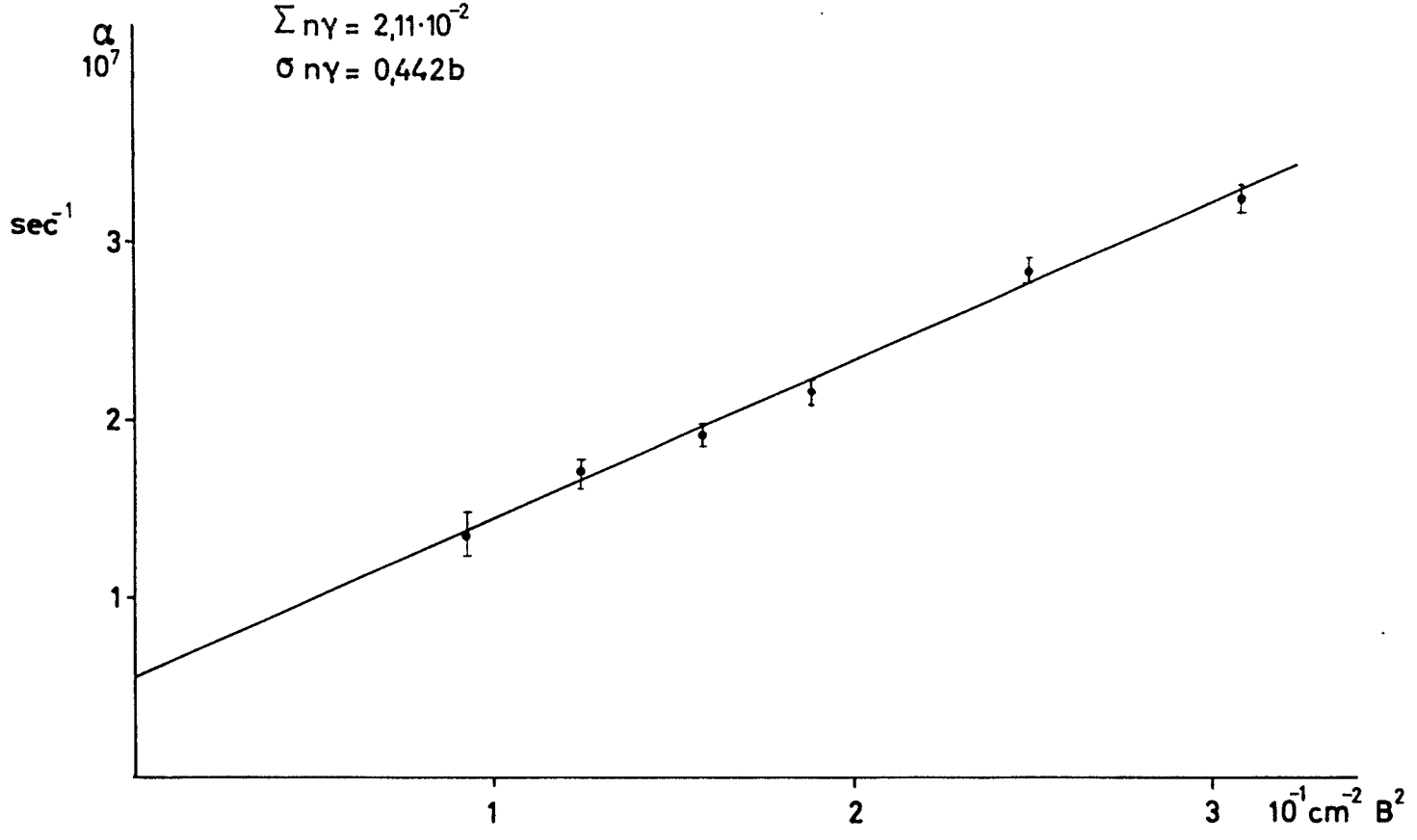

Fig. 12 α vs. B^2 curve for 30 keV neutrons in natural uranium